HHS Public Access

Author manuscript

J Cataract Refract Surg. Author manuscript; available in PMC 2016 April 29.

Published in final edited form as:

J Cataract Refract Surg. 2014 June ; 40(6): 991–998. doi:10.1016/j.jcrs.2014.04.013.

Biomechanics of corneal ectasia and biomechanical treatments

Cynthia J. Roberts, PhD and **William J. Dupps Jr, MD, PhD**

Department of Ophthalmology and Visual Science (Roberts), Department of Biomedical Engineering, The Ohio State University, Columbus, the Cole Eye Institute and Department of Biomedical Engineering (Dupps), Lerner Research Institute, Cleveland Clinic, and the Department of Biomedical Engineering (Dupps), Case Western Reserve University, Cleveland, Ohio, USA

Abstract

Many algorithms exist for the topographic/tomographic detection of corneas at risk for post-refractive surgery ectasia. It is proposed that the reason for the difficulty to find a universal screening tool based on corneal morphologic features is that curvature, elevation, and pachymetric changes are all secondary signs of keratoconus and post-refractive surgery ectasia and that the primary abnormality is in the biomechanical properties. It is further proposed that the biomechanical modification is focal in nature, rather than a uniform generalized weakening, and that the focal reduction in elastic modulus precipitates a cycle of biomechanical decompensation that is driven by asymmetry in the biomechanical properties. This initiates a repeating cycle of increased strain, stress redistribution, and subsequent focal steepening and thinning. Various interventions are described in terms of how this cycle of biomechanical decompensation is interrupted, such as intrastromal corneal ring segments, which redistribute the corneal stress, and collagen crosslinking, which modifies the basic structural properties.

Ectasias are characterized by progressive distortion of corneal curvature, which is thought to be associated with a “weaker” cornea. Conceptual models of keratoconus pathogenesis have evolved considerably in recent years and have postulated that keratocyte apoptosis[1] and abnormal regulation of collagenase, protease, and tissue inhibitors of matrix metalloproteinases-1 and-3[2] may play roles in the development of stromal ultrastructural abnormalities such as aberrant collagen organization,[3] loss of anchoring collagen fibrils near Bowman layer,[4] and stromal thinning. At the clinical level, rapid evolution of corneal

Corresponding author: Cynthia J. Roberts, PhD, 915 Olentangy River Road, Suite 5000, Columbus, Ohio 43212, USA. roberts.8@osu.edu.

Ashraf M. Mahmoud, BS, Abhijit Sinha Roy, PhD, Matthew R. Ford, BS, and Gunther Grabner, MD, contributed to the elastography experiment.

Financial Disclosures

Dr. Roberts is a consultant to Oculus, Inc., and Ziemer Ophthalmic Systems AG and has received research funding from Carl Zeiss Meditec AG, as well as travel funds from Sooft Italia. Dr. Dupps is listed as an inventor on intellectual property held by Cleveland Clinic related to biomechanical measurement and modeling and has received research funding and royalties from Avedro, Inc., Carl Zeiss Medite AG, and Topcon Medical Systems, Inc. related to the use of this intellectual property. Dr. Dupps is a consultant to Ziemer Ophthalmic Systems AG.

imaging technology has led to progress in the geometric characterization of keratoconus. However, the biomechanical features of keratoconus, which must comprise the final common pathway between molecular, genetic, and environmental factors and the clinical shape changes that lead to visual disability, have garnered little attention until recently. Studies of corneal tissue isolated from keratoconus patients in the 1970s and early 1980s revealed bulk abnormalities in mechanical strength and extracellular matrix constituents,[5–8] but progress in relating biomechanical properties to the clinical condition and its diagnosis or treatment has been limited by the lack of tools for measuring biomechanical properties in a clinical setting.

ECTASIA DEVELOPMENT AND DETECTION

The etiology of ectasia after excimer laser ablation is thought to be a loss of structural integrity of the cornea due to excess tissue removal leading to low residual stromal bed (RSB) thickness or, alternatively, the presence of undetected subclinical keratoconus preoperatively with the cornea in a weakened state prior to tissue removal. The earliest report of ectasia after laser in situ keratomileusis (LASIK) was in 1998, and it was postulated that corneas with forme fruste keratoconus might have altered biomechanical properties compared with normal corneas, along with a discussion of the importance of RSB in the etiology of ectasia.[9] A subsequent study confirmed the importance of the RSB, as well as attempted correction, as factors that may contribute to the occurrence of post-LASIK ectasia in a small series of patients.[10] However, without the ability to measure biomechanical properties directly, algorithm development for preoperative evaluation had to rely on available data. Classic methods for screening eyes for the presence of keratoconus preoperatively were based on anterior surface curvature irregularity from Placido topography[11–14] and were introduced early in the evolution of refractive surgery, including sophisticated neural network approaches fed with Placido-derived data.[15] Early reports of postoperative ectasia with clinical data such as level of myopia, total corneal thickness, and predicted RSB thickness[16] led to recommended preoperative screening for at risk corneas, in combination with anterior surface data.[17–21] The development of new scanning-slit and Scheimpflug tomographic devices allowed the addition of anterior and posterior elevation data to preoperative screening parameters,[22–25] as well as pachymetric profiles and volumetric data.[26,27] Corneal wavefront aberrations have been suggested,[28] as well as high-frequency ultrasound epithelial thickness mapping.[29] Various combinations of clinical findings, anterior curvature irregularity, thin pachymetry, atypical pachymetry profile, as well as posterior surface elevation anomalies, have been tried, but none has been totally effective in differentiating mildly pathologic corneas from those that are normal in a robust fashion. In fact, post-refractive-surgery ectasia has been reported in cases of apparently adequate corneal thickness, unremarkable curvature patterns, posterior surface elevation patterns within normal limits, and low amounts of ablation.[30,31]

We propose that the reason for the failure to find a universal screening tool based on corneal geometric features is that curvature, elevation, and pachymetric changes are secondary signs of keratoconus and that the earliest initiating changes occur in the biomechanical properties. We further propose that the initial biomechanical modification is focal in nature, rather than a uniform global weakening, and that the focal reduction in elastic modulus precipitates a

cycle of biomechanical decompensation. Although bulk viscoelastic biomechanical parameters have been proposed as an adjunct to both clinical findings and topographic/tomographic parameters in detecting corneas at risk for ectasia,[32] there is substantial overlap between normal corneas and keratoconic corneas in these parameters,[33,34] and they have not been as effective as anticipated. We hypothesize that bulk biomechanical assessment may not be sufficient to fully characterize an asymmetric disease. Spatial location of focal weakening in the cornea may be necessary to detect the disease at its earliest stages as well as fully characterize the progression.

BIOMECHANICAL CYCLE OF DECOMPENSATION IN ECTASIA

Biomechanical stress is represented as a force per unit area, and biomechanical strain is defined as deformation or stretching that can be expressed as percentage change in length. The elastic modulus of a material can be expressed as the slope of its stress–strain relationship. Therefore, a material that has a lower elastic modulus will deform or stretch more under the same load than a stiffer material with a higher elastic modulus. This is illustrated in the schematic stress–strain diagram in Figure 1 for a nonlinearly elastic material such as the cornea. Changes in geometry also affect the distribution of stress in the cornea. Thinner and flatter areas are associated with higher stress than thicker areas with greater curvature. If the cornea has a weak area, characterized by a lower elastic modulus that is surrounded by tissue with a higher elastic modulus, the weak area will deform to a greater extent when loaded by the intraocular pressure (Figure 2). This greater deformation can result in thinning of the tissue as it stretches in much the same way that a rubber band will thin as it stretches, as described by a material property known as the Poisson ratio. Biological responses to the changes in stress distribution may also contribute to thinning and localized reduction in elastic strength. As the cornea thins, the stress distribution becomes more asymmetric and the cornea deforms in the thinner higher stress region in a compensatory fashion to reduce the local stress by increasing the curvature. This results in further thinning, further modulation of the stress distribution, and further deformation, especially if the weak region becomes even weaker. This cyclic cascade of biomechanical decompensation results in clinical disease progression (Figure 3); ie, it is the disparity in biomechanical properties that likely drives the biomechanical progression in keratoconus rather than overall weakening. The bulk reduction in elastic modulus is probably characterized by disparity in the spatial distribution of biomechanical properties with a minimum in the area of the cone.

The question of whether keratoconus represents a true ectasia (involving stretching of tissue) as opposed to a warpage condition (with conservation of surface area) has been raised. In a study using surface area derivations based on Placido-based topography, Smolek and Klyce[35] found no significant differences in anterior corneal surface area in comparisons of normal post-photorefractive keratectomy (PRK) eyes and keratoconic eyes. While the lack of a significant difference between normal eyes and mild to moderate keratoconus argues for a relative large-scale conservation of surface area outside of advanced disease, it does not preclude the presence of local microstrain in a focally weak area that is not readily detected in a whole-surface analysis subject to the statistical limitations of sample size and variance. In serial finite element modeling simulations of ectasia progression that are not limited by

measurement variation, small but detectable increases in overall surface area that result from larger strains in the area of lowest elastic strength have been shown.[36] Keratoconus therefore most likely cannot be explained by rigid categorization into either ectasia or warpage; it probably represents both a local ectatic process with microstrain in areas of lower elastic strength and a relative macro-conservation of surface area that allows compensatory flattening of the extraconal cornea.

What could be the cause of focal weakening in the cornea? Perhaps pathologic tissue changes are initiated in a particular region of the cornea via a genetic predisposition. Perhaps an environmental factor is required to induce an abnormal phenotypical expression in the presence of a genetic lesion. It may be that repeated eye rubbing produces a focal area of weakening due to mechanical fatigue, similar to the repeated twisting of a paper clip leading to deformation and breakage, or it may be that eye rubbing acts as a trigger that alters gene expression. More research is needed to answer these questions. However, from a mechanical point of view, asymmetric thickness and curvature changes are easily explained by an asymmetric biomechanical property distribution and are difficult to explain otherwise.

FINITE ELEMENT BIOMECHANICAL MODELING OF ECTASIA

Theoretical analysis with finite element models of the corneal response to thinning and reduction of elastic modulus support the hypothesis of focal weakening. An early finite element model of keratoconus investigated thinning alone and found greater forward displacement with greater thinning, as well as an asymmetric response with a decentered thin region.[37] A later corneal finite element model of keratoconus investigated the loading response to a combination of thinning and reduction in elastic modulus.[38] The introduction of eccentric thinning was required to produce asymmetric displacement and an eccentric peak in dioptric curvature value if a normal elastic modulus was used. However, thinning alone was insufficient to cause dioptric values consistent with clinical cases of keratoconus with similar geometry. When eccentric thinning and reduced modulus were combined, the greatest forward displacement and peak dioptric values were produced, and it was concluded that both are involved in a complex relationship in the pathogenesis of keratoconus. From this type of modeling, however, it is not possible to determine whether corneal thinning or the reduction in elastic modulus occurs first and there was no attempt to model disease progression.

A whole-eye finite element model has been developed[39,40] that was modified to study keratoconus using corneal tomographic data from clinical cases (Figure 4).[36] To investigate the role of focal material weakness in the genesis of ectatic disease and its progression, the geometry of a topographically normal eye of a keratoconic subject with manifest keratoconus in the other eye was modeled. To simulate progression, the elastic modulus was reduced focally in an incremental manner to the same extent measured in extensiometric testing by Andreassen et al.[7] Curvature increased nonlinearly in the zone of material weakness from 44.0 diopters (D) to 52.0 D with a 45% decrease in modulus and resulted in focal steepening similar to that present in the more affected eye[36] (Figure 5). The results of this study are consistent with the hypothesis presented and demonstrated that progressive

reductions in elastic modulus were sufficient—without accompanying reductions in thickness—to reproduce the clinical topographic phenotype of keratoconus.

FOCAL WEAKENING IN ECTASIA: EXPERIMENTAL EVIDENCE

Does evidence of an asymmetric pattern of biomechanical properties in keratoconus exist other than the theoretical explanation and supporting finite element models? In a previously unpublished experiment, the authors investigated the spatial biomechanical properties of a keratoconic corneal button. The button had been removed during penetrating keratoplasty procedures and frozen for later analysis. Each button was marked with an identification number to allow it to be matched to the preoperative topography. The buttons were gradually thawed to room temperature in dextran prior to preliminary experiments. A Barron artificial anterior chamber was modified to hold an 8.0 mm corneal button, as shown in Figure 6, *A*. The region of exposed corneal tissue was 6.0 mm in diameter. The buttons were mounted securely in the chamber and pressurized to 10 mm Hg. The spatially resolved strain response of these buttons was measured using optical coherence elastography.[41] This system allows strain visualization across the 3-dimensional volume of the cornea. Figure 6, *B* and *C* show the preoperative corneal mires and the corresponding mires measured on the 8.0 mm button, respectively. Figure 7 shows the resulting strain map through the meridian containing the cone, which highlights a weaker area with reduced elastic modulus in the area of the topographic cone. In a series of experiments in human donor corneoscleral explants, Hong et al.[42] demonstrated that focal stromal weakening with collagenase produced mean increases in curvature and higher-order aberrations with morphology similar to keratoconus; in the same report, they showed that subsequent collagen crosslinking (CXL) produced opposite effects. These studies strongly support the hypothesis that keratoconus is dependent on an asymmetric distribution of corneal biomechanical properties. Validation in clinical keratoconus is an important impetus for rapid development of tools for clinical characterization of spatial properties.

The histopathological and ultrastructural differences between post-LASIK ectasia, post-PRK ectasia, and keratoconic corneas have been described based on the analysis of donor corneas for post-LASIK and post-PRK ectasia and corneal buttons after penetrating keratoplasty for keratoconus.[43] Similar features were found in all 3 ectasias in terms of fewer and thinner than normal lamellae in the region of ectasia. However, these changes were only present in the stress-bearing areas of the corneas with post-refractive surgery ectasia, which includes only the RSB in post-LASIK corneas and through the whole cornea depth after PRK. The breaks in Bowman layer seen in the keratoconic corneas were not relevant in eyes after refractive surgery, since this layer is nonexistent after PRK and within the low-stress bearing flap after LASIK. The cohesive tensile strength in corneas with keratoconus showed an area of focal weakening corresponding to the area of ectasia and located in the posterior two-thirds of the cornea. Other corneal depths in keratoconus were similar to normal corneas in their response. The ectatic corneas after refractive surgery could not be evaluated for cohesive tensile strength due to preservation prior to the study.[43] However, it is important to remember that the thinning seen in post-LASIK and post-PRK ectasia is, at least in part, due to tissue removal that has not occurred in keratoconus. This points to a structural difference despite similarities in the appearance of the lamellae themselves and surface topography. In

addition, in post-LASIK and post-PRK states, the anterior corneal stroma has been ablated, which represents the strongest region of the central cornea in terms of depth.[44] Therefore, biomechanically, these ectasias are all distinct and would not be expected to respond similarly to biomechanical treatments, such as intrastromal corneal ring segments (ICRS) placement and/or CXL.

BIOMECHANICAL TREATMENT OF ECTASIA

Topographic similarities and ultrastructural similarities between the ectasias do not necessarily imply biomechanical response similarities. One might expect the postrefractive-surgery ectasias to have greater variability in response to a biomechanical treatment than keratoconus due to the variability in width, depth, and the presence or absence of a flap in the excimer ablation procedures that were initially performed. This greater variability in response to treatment has been reported[45] as has a difference in thickness recovery time after CXL, with post-refractive surgery ectasia being more rapid than keratoconus.[46] Recognition of the biomechanical disparity in ectasia may lead to more effective treatment protocols. For example, CXL has been described to stiffen the keratoconic cornea by instilling riboflavin in combination with exposure to an ultraviolet-A light source.[47] The procedure was originally designed to halt progression of keratoconus, but has also been shown to improve visual acuity and reduce the magnitude of the maximum corneal curvature.[45] Corneal CXL currently involves the all-over treatment of an 8 to 9 mm diameter region of the cornea. However, if biomechanical disparity is characteristic of keratoconus, a nonuniform treatment might strengthen the cone to a greater extent than the surrounding areas of the cornea, thus reducing the proposed disparity. This would involve a targeted treatment in the area of the cone, with lesser treatment of the remaining corneal regions. This might allow even greater viscoelastic drift toward a more regular corneal shape over time. Simulation of this concept and the results of various corneal CXL patterns in a whole-eye finite element model has demonstrated a differential response depending on the location of the cone, the depth of simulated treatment, and the distribution of stiffening treatment relative to the cone location.[36] Specifically, greater magnitudes of flattening were achieved with focal increases in elastic modulus. Greater research is needed to optimize the biomechanical protocol, including the possibility of modeling the result prior to clinical treatment.

How do ICRS or targeted laser ablations interrupt the cycle of biomechanical decompensation? Intrastromal corneal ring segments will immediately redistribute the corneal stress by shortening lamellae and changing corneal shape without altering intrinsic properties.[48] This alters the cycle and pattern of progressive decompensation and allows viscoelastic drift toward a more regular corneal shape over time.[49] Corneal ablation also serves to immediately redistribute the stress, provided it is done in the thicker regions displaced from the cone. Topography-guided ablation in keratoconus has been reported[50] with reduction in surface irregularity over 2 years after treatment while the fellow eye continued to progress.[51] Ablation over the cone would be biomechanically detrimental and potentially increase the rate of progression. However, ablation in the thicker and flatter regions, while protecting the cone, has the potential to interrupt the cycle of decompensation. The ablated regions would strain or deform more, becoming steeper, and generate a more regular corneal shape. This biomechanical approach is opposite to the

shape–subtraction model that is the basis of standard ablation profiles. In a shape–subtraction approach, ablating in the central area of greater curvature causes central flattening and corresponding peripheral steepening. In a biomechanical approach, ablating in the flatter regions causes local steepening with corresponding flattening in the nonablated areas of greater curvature. Combined treatments of ICRS implantation plus corneal CXL[52] or, alternatively, biomechanically targeted ablation plus corneal CXL[53–56] would link redistributing stress via ICRS or ablation with changing biomechanical properties via CXL. These combined treatments have the potential to provide even greater improvement in corneal shape over time, as the biomechanical cycle of decompensation is not only interrupted, but potentially reversed.

THE FUTURE

If a detection system to measure nonuniformity in biomechanical properties across the cornea and localize focal weakening could be developed, clinical evidence could be acquired to test the hypothesis presented. In addition, irregular curvature that is the result of pathology could be differentiated from an irregular curvature pattern that is a variant of normal in biomechanically normal corneas. This would be ideal in the effort to screen for at-risk patients to reduce the incidence of post-refractive-surgery ectasia, as well as to allow surgery to be performed in candidates with no underlying biomechanical pathology who might previously have been turned away because of topographic irregularity. It would also allow targeting of the weakest areas for customized targeted treatment in diagnosed keratoconus to reduce the proposed asymmetry in biomechanical properties. The authors are encouraged by the recent acceleration of research and development efforts in this important area.

Acknowledgments

Supported by the Ohio Lions Eye Research Foundation and Martha G. and Milton Staub Fund to the Department of Ophthalmology and Visual Science, The Ohio State University; National Institutes of Health R01 EY023381, an Ohio Third Frontier Innovation Platform Award from the State of Ohio to Cleveland Clinic Cole Eye Institute (TECH 13-059), the National Keratoconus Foundation/Discovery Eye Foundation, and unrestricted and challenge grants from Research to Prevent Blindness to the Department of Ophthalmology, Cleveland Clinic Lerner College of Medicine of Case Western Reserve University. Dr. Dupps is a recipient of a Research to Prevent Blindness Career Development Award.

REFERENCES

1. Kim W-J, Rabinowitz YS, Meisler DM, Wilson SE. Keratocyte apoptosis associated with keratoconus. Exp Eye Res. 1999; 69:475–481. [PubMed: 10548467]
2. Matthews FJ, Cook SD, Majid MA, Dick AD, Smith VA. Changes in the balance of the tissue inhibitor of matrix metalloproteinases (TIMPs)-1 and -3 may promote keratocyte apoptosis in keratoconus. Exp Eye Res. 2007; 84:1125–1134. [PubMed: 17449031]
3. Meek KM, Tuft SJ, Huang Y, Gill PS, Hayes S, Newton RH, Bron AJ. Changes in collagen orientation and distribution in keratoconus corneas. Invest Ophthalmol Vis Sci. 2005; 46:1948–1956. Available at: http://www.iovs.org/content/46/6/1948.full.pdf. [PubMed: 15914608]
4. Morishige N, Wahlert AJ, Kenney MC, Brown DJ, Kawamoto K, Chikama T-i, Nishida T, Jester JV. Second-harmonic imaging microscopy of normal human and keratoconus cornea. Invest Ophthalmol Vis Sci. 2007; 48:1087–1094. Available at: http://www.iovs.org/cgi/reprint/48/3/1087. [PubMed: 17325150]

5. Foster CS, Yamamoto GK. Ocular rigidity in keratoconus. Am J Ophthalmol. 1978; 86:802–806. [PubMed: 736078]
6. Cannon DJ, Foster CS. Collagen crosslinking in keratoconus. Invest Ophthalmol Vis Sci. 1978; 17:63–65. Available at: http://www.iovs.org/cgi/reprint/17/1/63. [PubMed: 621128]
7. Andreassen TT, Simonsen AH, Oxlund H. Biomechanical properties of keratoconus and normal corneas. Exp Eye Res. 1980; 31:435–441. [PubMed: 7449878]
8. Nash IS, Greene PR, Foster CS. Comparison of mechanical properties of keratoconus and normal corneas. Exp Eye Res. 1982; 35:413–424. [PubMed: 7173339]
9. Seiler T, Quurke AW. Iatrogenic keratectasia after LASIK in a case of forme fruste keratoconus. J Cataract Refract Surg. 1998; 24:1007–1009. [PubMed: 9682124]
10. Pallikaris IG, Kymionis GD, Astyrakakis NI. Corneal ectasia induced by laser in situ keratomileusis. J Cataract Refract Surg. 2001; 27:1796–1802. [PubMed: 11709254]
11. Wilson SE, Klyce SD. Screening for corneal topographic abnormalities before refractive surgery. Ophthalmology. 1994; 101:147–152. [PubMed: 8302548]
12. Maeda N, Klyce SD, Smolek MK, Thompson HW. Automated keratoconus screening with corneal topography analysis. Invest Ophthalmol Vis Sci. 1994; 35:2749–2757. Available at: http://www.iovs.org/cgi/reprint/35/6/2749.pdf. [PubMed: 8188468]
13. Rabinowitz YS. Videokeratographic indices to aid in screening for keratoconus. J Refract Surg. 1995; 11:371–379. [PubMed: 8528916]
14. Maeda N, Klyce SD, Smolek MK. Comparison of methods for detecting keratoconus using videokeratography. Arch Ophthalmol. 1995; 113:870–874. [PubMed: 7605277]
15. Smolek MK, Klyce SD. Current keratoconus detection methods compared with a neural network approach. Invest Ophthalmol Vis Sci. 1997; 38:2290–2299. Available at: http://www.iovs.org/cgi/reprint/38/11/229. [PubMed: 9344352]
16. Binder P. Ectasia after laser in situ keratomileusis. J Cataract Refract Surg. 2003; 29:2419–2429. [PubMed: 14709307]
17. Randleman JB, Russell B, Ward MA, Thompson KP, Stulting RD. Risk factors and prognosis for corneal ectasia after LASIK. Ophthalmology. 2003; 110:267–275. [PubMed: 12578766]
18. Randleman JB, Woodward M, Lynn MJ, Stulting RD. Risk assessment for ectasia after corneal refractive surgery. Ophthalmology. 2008; 115:37–50. [PubMed: 17624434]
19. Randleman JB, Trattler WB, Stulting RD. Validation of the Ectasia Risk Score System for preoperative laser in situ keratomileusis screening. Am J Ophthalmol. 2008; 145:813–818. [PubMed: 18328998]
20. Li X, Yang H, Rabinowitz YS. Keratoconus: classification scheme based on videokeratography and clinical signs. J Cataract Refract Surg. 2009; 35:1597–1603. [PubMed: 19683159]
21. Holladay JT. Keratoconus detection using corneal topography. J Refract Surg. 2009; 25:S958–S962. [PubMed: 19848378]
22. Rao SN, Raviv T, Majmudar PA, Epstein RJ. Role of Orbscan II in screening keratoconus suspects before refractive corneal surgery. Ophthalmology. 2002; 109:1642–1646. [PubMed: 12208710]
23. Ambrósio R Jr, Klyce SD, Wilson SE. Corneal topographic and pachymetric screening of keratorefractive patients. J Refract Surg. 2003; 19:24–29. [PubMed: 12553601]
24. Duffey RJ. Preoperative LASIK screening: an evolving standard of care [letter]. J Cataract Refract Surg. 2005; 31:1084–1085. [PubMed: 16039465]
25. Tabbara KF, Kotb AA. Risk factors for corneal ectasia after LASIK. Ophthalmology. 2006; 113:1618–1622. [PubMed: 16949446]
26. Ambrósio R Jr, Alonso RS, Luz A, Coca Velarde LG. Corneal-thickness spatial profile and corneal-volume distribution: tomographic indices to detect keratoconus. J Cataract Refract Surg. 2006; 32:1851–1859. [PubMed: 17081868]
27. Wolf A, Abdallat W, Kollias A, Fröhlich SJ, Grueterich M, Lackerbauer CA. Mild topographic abnormalities that become more suspicious on Scheimpflug imaging. Eur J Ophthalmol. 2009; 19:10–17. [PubMed: 19123143]
28. Jafri B, Li X, Yang H, Rabinowitz YS. Higher order wavefront aberrations and topography in early and suspected keratoconus. J Refract Surg. 2007; 23:774–781. [PubMed: 17985796]

29. Reinstein DZ, Archer TJ, Gobbe M. Stability of LASIK in topographically suspect keratoconus confirmed non-keratoconic by Artemis VHF digital ultrasound epithelial thickness mapping: 1-year follow-up. J Refract Surg. 2009; 25:569–577. [PubMed: 19662913]
30. Klein SR, Epstein RJ, Randleman JB, Stulting RD. Corneal ectasia after laser in situ keratomileusis in patients without apparent preoperative risk factors. Cornea. 2006; 25:388–403. [PubMed: 16670474]
31. Ambrósio R Jr, Dawson DG, Salomão M, Guerra FP, Caiado ALC, Belin MW. Corneal ectasia after LASIK despite low preoperative risk: tomographic and biomechanical findings in the unoperated, stable, fellow eye. J Refract Surg. 2010; 26:906–911. [PubMed: 20481412]
32. Fontes BM, Ambrósio R Jr, Salomão M, Velarde GC, Nosé W. Biomechanical and tomographic analysis of unilateral keratoconus. J Refract Surg. 2010; 26:677–681. [PubMed: 19928695]
33. Luce DA. Determining in vivo biomechanical properties of the cornea with an ocular response analyzer. J Cataract Refract Surg. 2005; 31:156–162. [PubMed: 15721708]
34. Schweitzer C, Roberts CJ, Mahmoud AM, Colin J, Maurice-Tison S, Kerautret J. Screening of forme fruste keratoconus with the Ocular Response Analyzer. Invest Ophthalmol Vis Sci. 2010; 51:2403–2410. Available at: http://www.iovs.org/content/51/5/2403.full.pdf. [PubMed: 19907025]
35. Smolek MK, Klyce SD. Is keratoconus a true ectasia? An evaluation of corneal surface area. Arch Ophthalmol. 2000; 118:1179–1186. Available at: http://archopht.jamanetwork.com/data/Journals/OPHTH/9878/ecs80115.pdf. [PubMed: 10980762]
36. Sinha Roy A, Dupps WJ Jr. Computational modeling of keratoconus progression and differential responses to collagen crosslinking. Invest Ophthalmol Vis Sci. 2011; 52:9174–9187. Available at: http://www.iovs.org/content/52/12/9174.full.pdf. [PubMed: 22039252]
37. Anderson K, El-Sheikh A, Newson T. Application of structural analysis to the mechanical behavior of the cornea. J R Soc Interface. 2004; 1:3–15. Available at: http://www.ncbi.nlm.nih.gov/pmc/articles/PMC1618927/pdf/16849148.pdf. [PubMed: 16849148]
38. Gefen A, Shalom R, Elad D, Mandel Y. Biomechanical analysis of the keratoconic cornea. J Mech Behav Biomed Mater. 2009; 2:224–236. [PubMed: 19627827]
39. Sinha Roy A, Dupps WJ Jr. Effects of altered corneal stiffness on native and postoperative LASIK corneal biomechanical behavior: a whole-eye finite element analysis. J Refract Surg. 2009; 25:875–887. [PubMed: 19835328]
40. Sinha Roy A, Dupps WJ Jr. Patient-specific modeling of corneal refractive surgery outcomes and inverse estimation of elastic property changes. J Biomech Eng. 2011; 133:011002. [PubMed: 21186892]
41. Ford MR, Dupps WJ Jr, Sinha Roy S, Rollins AM, Hu Z. Method for optical coherence elastography of the cornea. J Biomed Opt. 2011; 16:016005. Available at: http://www.ncbi.nlm.nih.gov/pmc/articles/PMC3041813/pdf/JBOPFO-000016-016005_1.pdf. [PubMed: 21280911]
42. Hong CW, Sinha-Roy A, Schoenfield L, McMahon JT, Dupps WJ Jr. Collagenase-mediated tissue modeling of corneal ectasia and collagen cross-linking treatments. Invest Ophthalmol Vis Sci. 2012; 53:2321–2327. Available at: http://www.iovs.org/content/53/4/2321.full.pdf. [PubMed: 22427568]
43. Dawson DG, Grossniklaus HE, McCarey BE, Edelhauser HF. Biomechanical and wound healing characteristics of corneas after excimer laser keratorefractive surgery: is there a difference between advanced surface ablation and sub-Bowman's keratomileusis? J Refract Surg. 2008; 24:S90–S96. [PubMed: 18269157]
44. Randleman JB, Dawson DG, Grossniklaus HE, McCarey BE, Edelhauser HF. Depth-dependent cohesive tensile strength in human donor corneas: implications for refractive surgery. J Refract Surg. 2008; 24:S85–S89. [PubMed: 18269156]
45. Hersh PS, Greenstein SA, Fry KL. Corneal collagen crosslinking for keratoconus and corneal ectasia: one-year results. J Cataract Refract Surg. 2011; 37:149–160. [PubMed: 21183110]
46. Greenstein SA, Shah VP, Fry KL, Hersh PS. Corneal thickness changes after corneal collagen crosslinking for keratoconus and corneal ectasia: one-year results. J Cataract Refract Surg. 2011; 37:691–700. [PubMed: 21420594]

47. Wollensak G, Spoerl E, Seiler T. Riboflavin/ultraviolet-A–induced collagen crosslinking for the treatment of keratoconus. Am J Ophthalmol. 2003; 135:620–627. Available at: http://grmc.ca/assets/files/collagen_crosslinking_2003_wollensak.pdf. [PubMed: 12719068]

48. Dauwe C, Touboul D, Roberts CJ, Mahmoud A, Kérautret J, Fournier P, Malecaze F, Colin J. Biomechanical and morphological corneal response to placement of intrastromal corneal ring segments for keratoconus. J Cataract Refract Surg. 2009; 35:1761–1767. [PubMed: 19781473]

49. Roberts, CJ. Biomechanics of INTACS in keratoconus. In: Colin, J.; Ertan, A., editors. Intracorneal Ring Segments and Alternative Treatments for Corneal Ectatic Diseases. Ankara Turkey, Kudret Eye Hospital; 2007. p. 157-166.

50. Tamayo Fernandez GE, Serrano MG. Early clinical experience using custom excimer laser ablations to treat irregular astigmatism. J Cataract Refract Surg. 2000; 26:1442–1450. [PubMed: 11033389]

51. Cennamo G, Intravaja A, Boccuzzi D, Marotta G, Cennamo G. Treatment of keratoconus by topography-guided customized photorefractive keratectomy: two-year follow-up study. J Refract Surg. 2008; 24:145–149. [PubMed: 18297938]

52. Kamburoglu G, Ertan A. Intacs implantation with sequential collagen cross-linking treatment in postoperative LASIK ectasia. J Refract Surg. 2008; 24:S726–S729. [PubMed: 18811119]

53. Kanellopoulos AJ. Comparison of sequential vs same-day simultaneous collagen cross-linking and topography-guided PRK for treatment of keratoconus. J Refract Surg. 2009; 25:S812–S818. [PubMed: 19772257]

54. Kymionis GD, Kontadakis GA, Kounis GA, Portaliou DM, Karavitaki AE, Magarakis M, Yoo S, Pallikaris IG. Simultaneous topography-guided PRK followed by corneal collagen cross-linking for keratoconus. J Refract Surg. 2009; 25:S807–S811. [PubMed: 19772256]

55. Krueger RR, Kanellopoulos AJ. Stability of simultaneous topography-guided photorefractive keratectomy and riboflavin/UVA cross-linking for progressive keratoconus: case reports. J Refract Surg. 2010; 26:S827–S832. [PubMed: 20954679]

56. Stojanovic A, Zhang J, Chen X, Nitter TA, Chen S, Wang Q. Topography-guided transepithelial surface ablation followed by corneal collagen cross-linking performed in a single combined procedure for the treatment of keratoconus and pellucid marginal degeneration. J Refract Surg. 2010; 26:145–152. [PubMed: 20163079]

Synopsis

The basics of biomechanical properties are described, along with proposed sources for biomechanical progression in various ectasias, including how progression might be interrupted with interventions such as crosslinking and intrastromal rings.

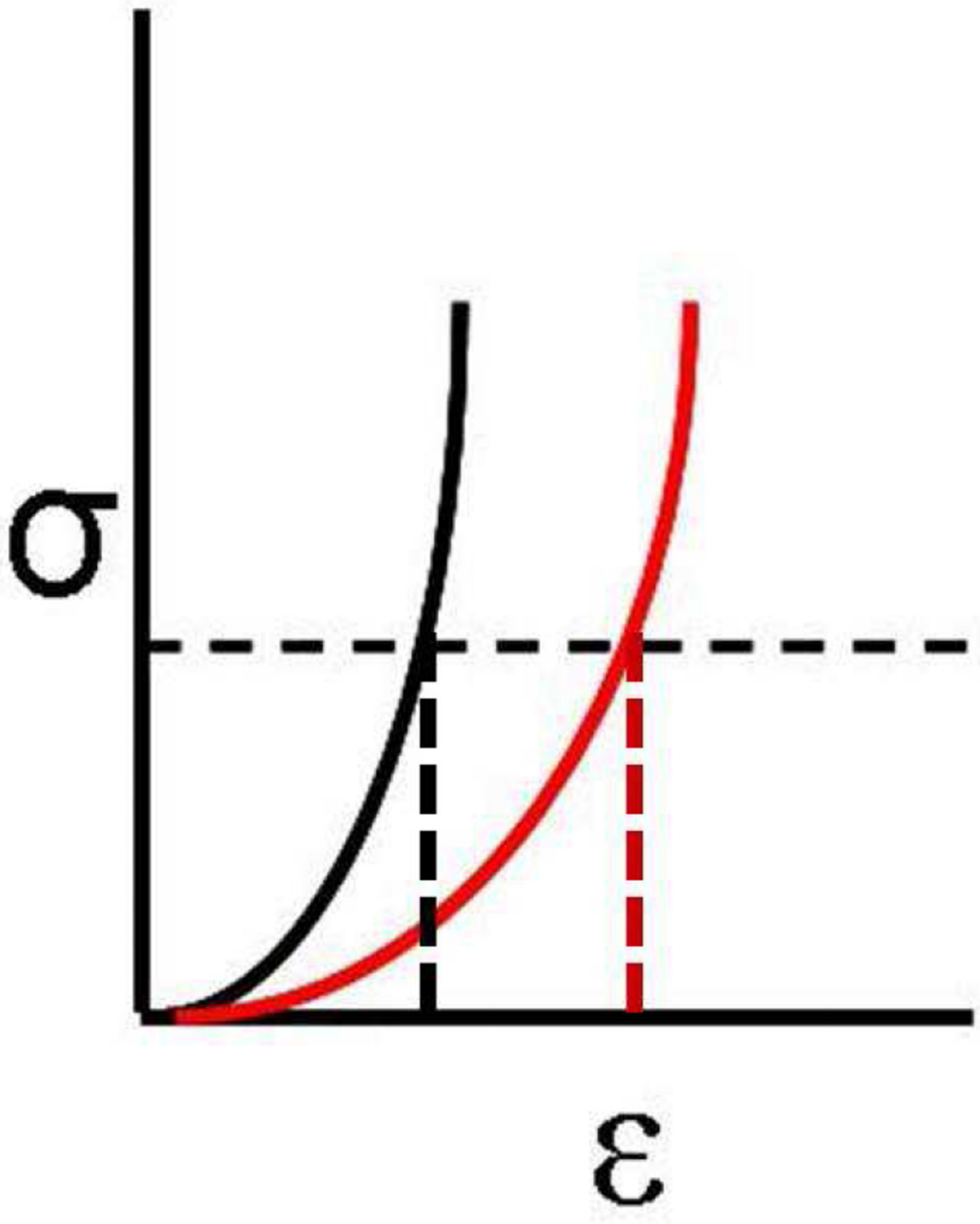

Figure 1.

Stress (σ) on the *y*-axis is defined as force over cross-sectional area and strain (ε) on the *x*-axis is defined as percent change in length. A constant stress horizontal dashed line is shown. A higher elastic modulus material (*black*) will have less strain or less deformation than a lower elastic modulus material (*red*) at the same stress, as shown by the vertical dashed lines.

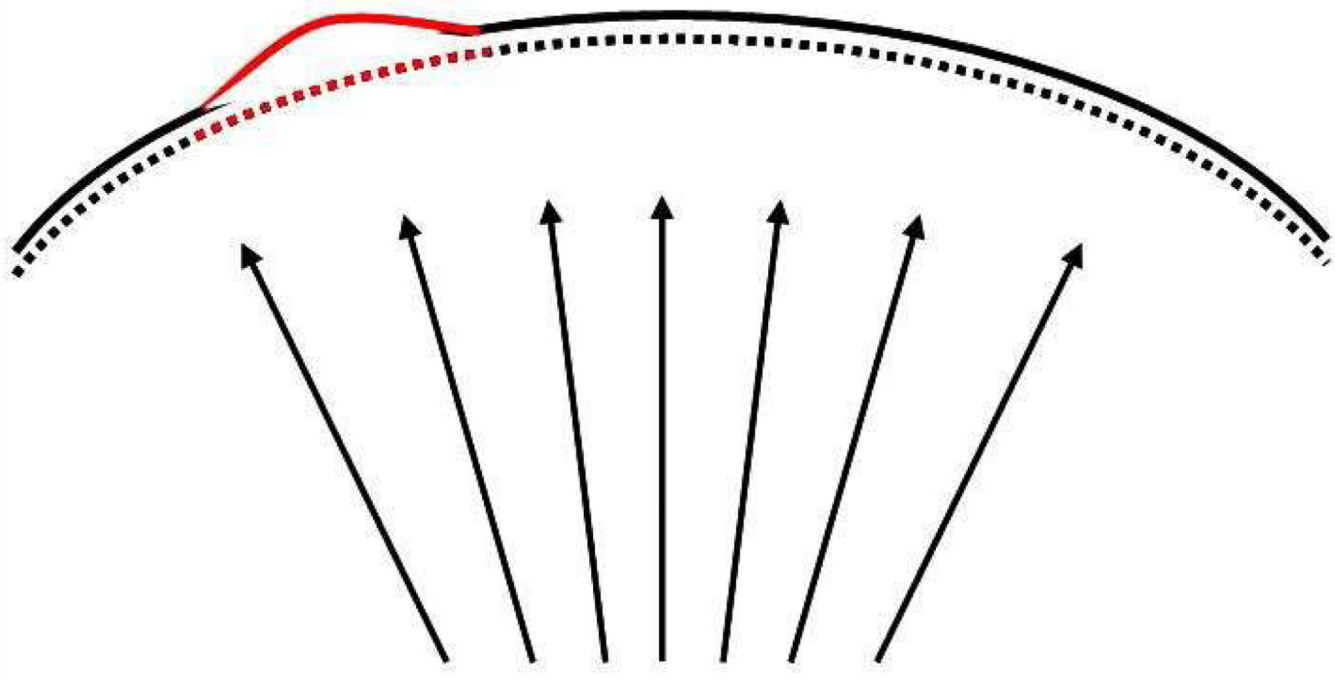

Figure 2.

Cornea with a focally weak area of lower elastic modulus (*red*) surrounded by areas of higher elastic modulus (*black*) will strain to a greater extent when placed under the same intraocular pressure load. Greater deformation occurs in the weaker region, which is exaggerated for illustration.

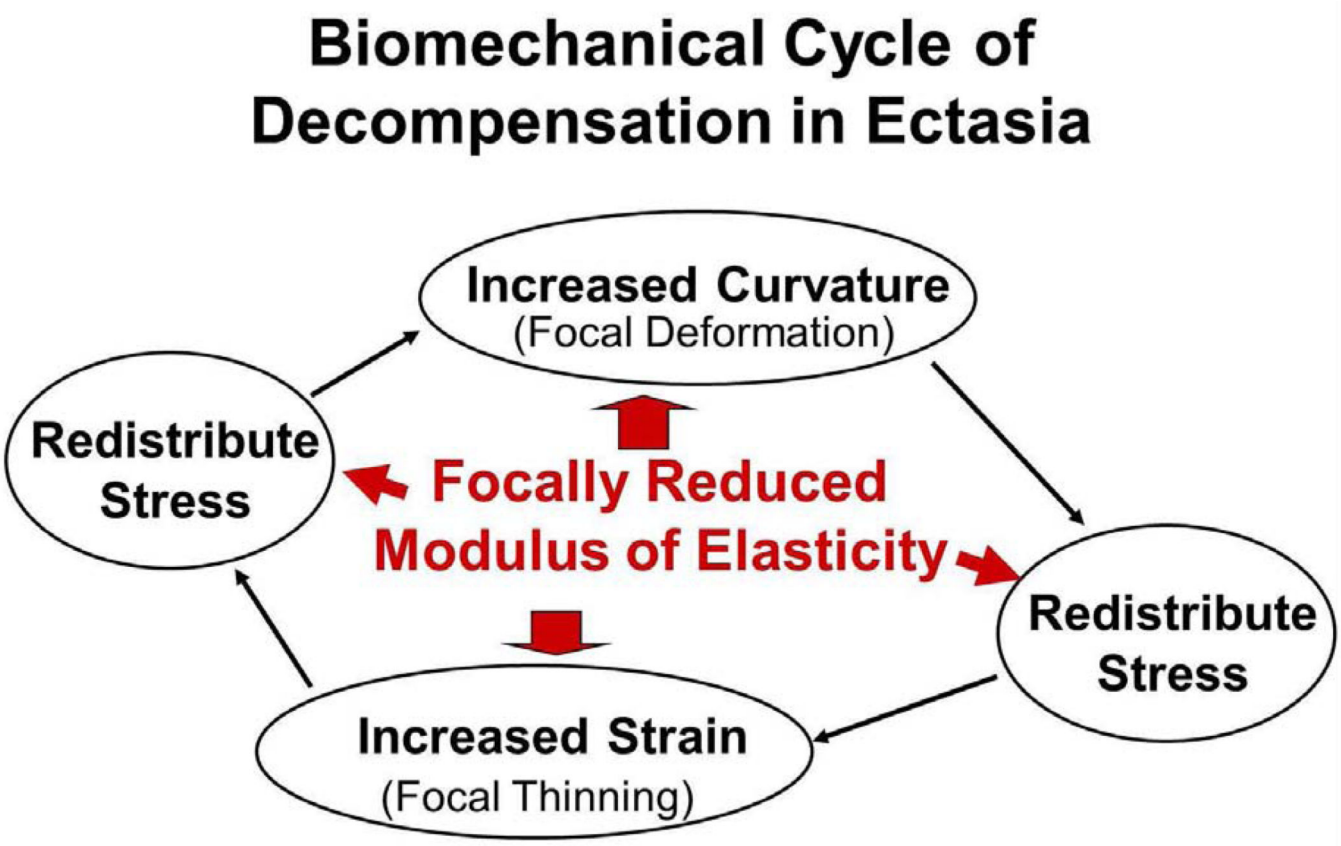

Figure 3.

Proposed schematic for a biomechanical cycle of decompensation in ectasia. The cycle is initiated by asymmetry in the distribution of biomechanical properties, which causes the cornea to thin, which causes an increase in stress, which causes the cornea to deform or redistribute curvature in a compensatory fashion.

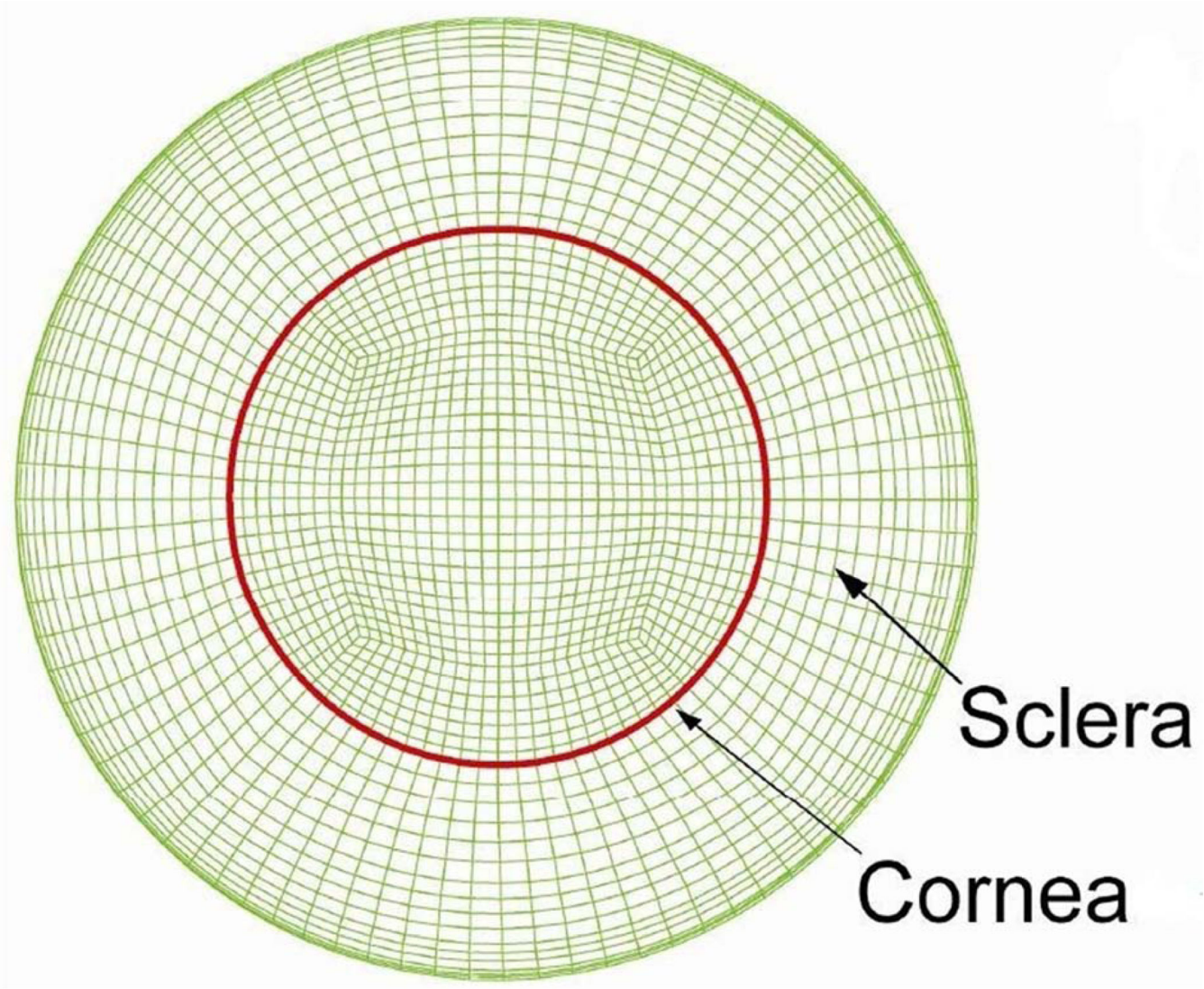

Figure 4.
Example of mesh from a 3-dimensional whole-eye finite element model that has been modified to evaluate progression in keratoconus.

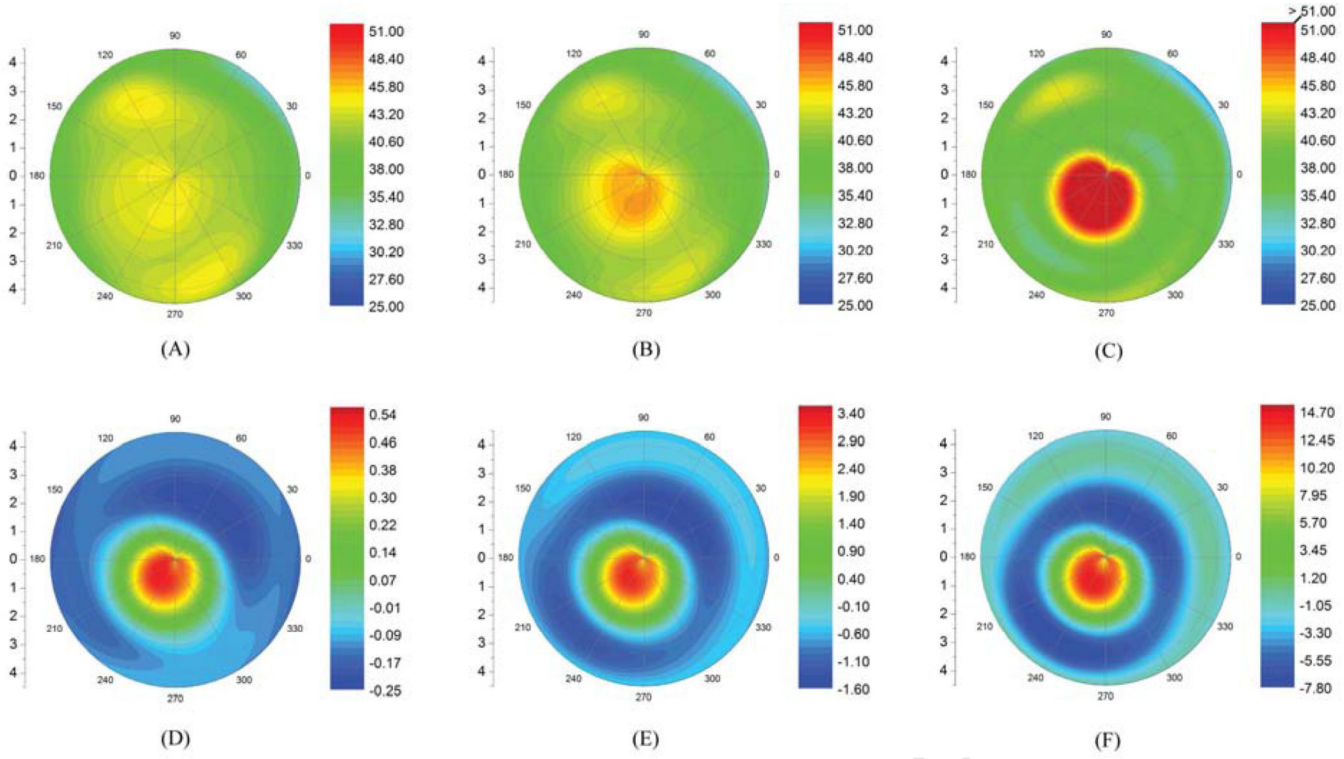

Figure 5.

Finite element model-generated tangential curvature maps of the anterior corneal surface of the less affected eye of an asymmetric keratoconus patient after elastic modulus reductions of (*A*) 10%, (*B*) 30%, and (*C*) 45%. *D* to *F*: Associated tangential curvature difference maps for each elastic modulus decrement (Reprinted with permission of Investigative Ophthalmology & Visual Science[36])

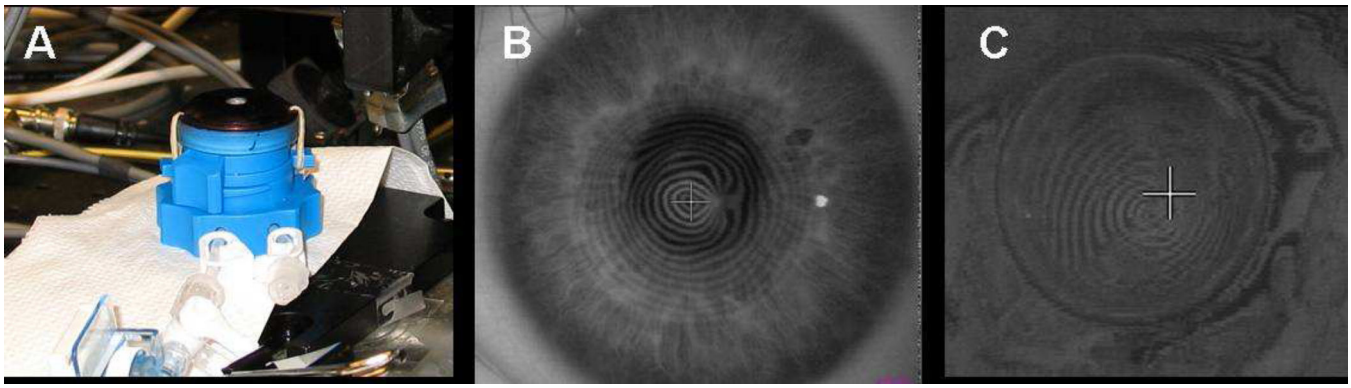

Figure 6.

A: Modified artificial anterior chamber to hold 8 mm corneal button with 6 mm of exposed tissue. *B*: Preoperative topographic mires measured with Keratron. *C*: Topographic mires of thawed keratoconic button of same patient in mount for cone localization with pressure of 10 mm Hg measured with a Keratron Scout.

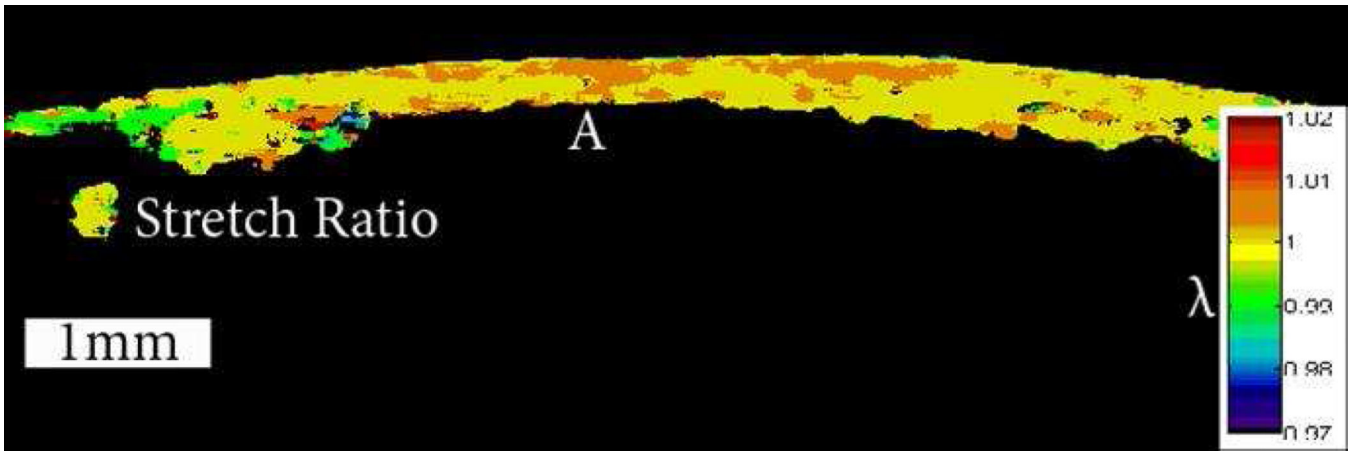

Figure 7.

Axial stretch ratio under a change in pressure of 10 mm Hg. The tissue above the label A was identified as the cone on the Keratron scout and the optical coherence tomography images. Portions of the stroma and tissue with low cross-correlation coefficients are not shown. The cone demonstrates the highest concentration of strain and the lowest resistance to deformation.